Some numerical simulations of large deformations of heterogeneous hyperelastic media

Philippe Aubert, Christian Licht, Stéphane Pagano

Some numerical simulations of large deformations of heterogeneous hyperelastic media

Philippe Aubert · Christian Licht · Stéphane Pagano

Abstract Numerical experiments done on a two-dimensional stratified two-phase composite corroborate theoretical results on homogeneization of media capable of large deformations.

Keywords Homogenization · Large deformations · Non-convex energy density

1 Introduction

Determining the behaviour of a structure made of a highly heterogeneous hyper-elastic material is a rather difficult numerical problem. The homogenization theory, whose purpose is to determine the macroscopic behaviour of such materials, may provide some help. In some cases of periodic heterogeneity distribution, macroscopic behaviour is that of a homogeneous material, with an explicit expression of the homogenized bulk energy density. The well-known formula derived in the seventies [2,9,13–15] for linearly elastic media also works in the case of convex energy densities [10] that satisfy the growth conditions:

$$\begin{aligned}&\exists\quad p>1\quad \exists\quad a,b>0\quad such\quad that\\ &a\,|F|^p \le W(y,F) \le b(1+|F|^p)\quad \forall F\in M_d, \forall y\in Y\end{aligned}\tag{1}$$

where F is the deformation gradient, M_d the set of $d\times d$ matrices, d (= 2 or 3) the space dimension and Y the basic cell which describes the periodicity of the medium. The homogenized density reads as:

$$W^{hom}(F)=inf\left\{\frac{1}{|Y|}\int_Y W(y,F+\nabla\psi)dy,\ \psi\in V_{per}(Y)\right\}\tag{2}$$

where $|Y|$ is the volume (or area) of Y and V_{per} is the subspace of the Y-periodic fields of the Sobolev space $W^{1,p}(Y)^d$.

But it is well known [4] that the convexity of the stored energy is not suitable for the framework of large deformations. For non convex densities which satisfy the growth condition (1) and:

$$\begin{aligned}&\exists\quad c>0\quad such\quad that\\ &\left|W(y,F)-W(y,F')\right|\\ &\le c\left(1+|F|^{p-1}+\left|F'\right|^{p-1}\right)\left|F-F'\right|\quad \forall F,F'\in M_d\end{aligned}\tag{3}$$

Braides [3] and Müller [11] have established that the homogenized energy density is given by:

$$\begin{aligned}&W^{hom}(F)=inf\{W^n(F);\,n=1,2,3,...\}\\ &with\quad W^n(F)=inf\left\{\frac{1}{|nY|}\int_{nY} W(y,F+\nabla\psi)dy,\ \psi\in V_{per}(nY)\right\}\end{aligned}\tag{4}$$

The difference between the expression (2) for convex W and the expression (4) for non convex W is considerable. For convex W, it is sufficient to consider fields which are periodic in one cell Y, so that Y is representative of the medium from both the geometrical and mechanical points of view. For non

P. Aubert · C. Licht · S. Pagano (✉)
LMGC, UMR CNRS 5508, Université Montpellier II,
CC048 Place Eugène Bataillon, 34095 Montpellier Cedex 5, France
e-mail: pagano@lmgc.univ-montp2.fr

convex density, the periodic fields must be considered for each nY set of n^d basic cells (Fig. 1). Hence, Y is representative of the medium from a purely geometrical point of view. Actually, the expression (4) allows one to consider deformation gradient oscillations at a finer scale than formula (2).

Unfortunately, the growth condition (1) is incompatible with the condition:

$$det(F) \to 0 \Rightarrow W(F) \to \infty, \tag{5}$$

which expresses the need for an infinite amount of energy to squeeze a block of matter down to a point. Thus, the homogenized density of a realistic heterogeneous hyperelastic medium is still unknown.

The aim of this paper is to illustrate these theoretical considerations by some numerical experiments. For instance, when local bucklings may occur the volume averaged strain energy (Formula (2)) can lead to significant errors by providing a far stronger homogeneized material. The experiments are carried out on a two-dimensional stratified two-phase composite material (Fig. 1).

More precisely, the unit cell Y is $(0, 1) \times (0, 1)$ and let $Q = (0, \frac{1}{2}) \times (0, 1)$ and

$$W(y, F) = \left\{\alpha \chi_Q(y) + \chi_{Y/Q}(y)\right\} w(F) \tag{6}$$

where:

- χ_Q, $\chi_{Y/Q}$ are the characteristic functions of Q and Y/Q
- α represents the relative strength of the two-phase and is equal, here, to 10^6 to give a high contrast.
- w is a function chosen among $\{w_M, w_{CG}\}$

The non convex density w_M:

$$w_M(F) = |F|^4 + h(det(F)), \tag{7}$$
$$h(\delta) = \begin{cases} -\frac{76\delta+48}{5\delta+2} & \text{if } \delta > 0 \\ -98\delta + 24 & \text{if } \delta \le 0, \end{cases}$$

was introduced by Müller [11] to show the large discrepancy between the homogenized density formulae for convex

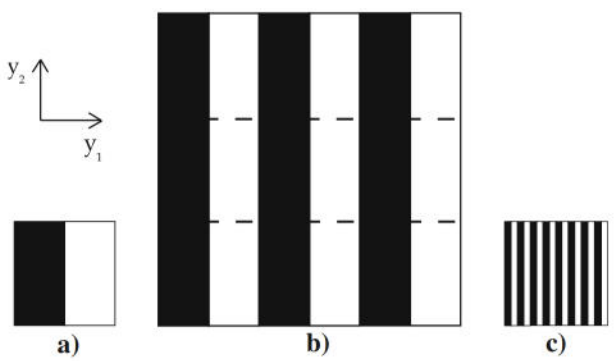

Fig. 1 **a** The unit cell Y, **b** the set $3Y$, **c** a unit sample of the composite when the density of the layers of each phase is 8

and non convex W. Whereas w_M does not satisfy (5), the so-called Ciarlet–Geymonat energy density [5]:

$$w_{CG}(F) = 0.505\left(|F|^2 - 2\right) + 0.355\left((det(F))^2 - 1\right) - 0.86\,\mathrm{Log}(det(F)), \tag{8}$$

belongs to the class of Ogden's densities which are often used to model several rubber-like solids.
To numerically tackle the problem:

$$(P_n)\ inf\left\{\frac{1}{|nY|}\int_{nY} W(y, F+\nabla\psi(y))\,dy,\ \ \psi \in V_{per}(nY)\right\}$$

related to (4), the Newton–Raphson algorithm was chosen, whose one iteration reads as:

$$\begin{cases} Find \quad \psi^{k+1} \in V^k_{per}(nY) \quad such \quad that \\ \\ \int_{nY} \frac{\partial^2 W(y, F+\nabla\psi^k)}{\partial F^2}\left(\nabla\psi^{k+1} - \nabla\psi^k\right)\nabla h\,dy \\ \quad = -\int_{nY} \frac{\partial W(y, F+\nabla\psi^k)}{\partial F}\nabla h\,dy, \forall h \in V^k_{per}(nY) \end{cases} \tag{9}$$

where $V^k_{per}(nY)$ is a "finite-element" subspace of $V_{per}(nY)$. In fact, the periodicity conditions are enforced by Lagrange multipliers [7,8]. In all the numerical experiments, the "convergence" test $|\psi^{k+1} - \psi^k| < 10^{-4}|\psi^k|$ has to be satisfied for five consecutive iterations.

The fundamental non convexity of the bulk energy implies that the "solution" supplied by the Newton–Raphson algorithm is close to a critical point of $I(\psi) = \int_{nY} W(y, F + \nabla\psi)dy$ and not necessary a minimum, even locally. The focus here is on macroscopic deformation gradients corresponding to contractions in the direction of the layers. It is intuitive that minima will present oscillations with respect to the y_2 "vertical" coordinate. To obtain a "solution" $\psi_{n,m}$ with m undulations the algorithm can be initialized with a field like $\psi^0_{n,p}(y) = (A(n)sin(\pi p y_2), 0)$. This method is very sensitive to the choice of $A(n)$: for instance, an initial guess with $p = 4$ can supply a deformation field with two undulations. Ultimately, an approximate solution of (P_n) is expected to be the field $\psi_{n,m_{opt}(n)}$ which minimizes:

$$m \in \mathbb{N} \to I_{n,m}(F) = \frac{1}{|nY|}\int_{nY} W(y, F + \nabla\psi_{n,m})dy$$

and we set:

$$\overline{I}_n(F) = I_{n,m_{opt}(n)}(F) \tag{10}$$

so that $\overline{I}_n(F)$ is a numerical approximation of $W^n(F)$. In the sequel the deformation associated with $\psi_{n,m}$, $\psi_{n,m_{opt}(n)}$ is denoted by $\varphi_{n,m}$ and $\overline{\varphi}_n$, respectively: $\varphi_{n,m}(y) = Fy + \psi_{n,m}(y)$, $\overline{\varphi}_n(y) = Fy + \psi_{n,m_{opt}(n)}(y)$.

2 Numerical experiments concerning the energy density W_M

Here, W_M is the energy density deduced from (6) with $w = w_M$.

2.1 Contraction in the direction of the layers

Here $F = \begin{pmatrix} 1 & 0 \\ 0 & d \end{pmatrix}$, $0 < d < 1$.

First, for $0.9 < d \leq 1$, the Newton–Raphson algorithm supplies a "solution" without undulation for every value of n ($m_{opt}(n) = 0$). Moreover $\overline{I}_n(F)$ does not depend on n. Thus, the homogenized energy density is obtained by a formula like (2).

For $0.74 \leq d \leq 0.9$, $I_{n,m}$ depends strongly on n and m: $I_{n,m}$ increases with m but is always smaller than $I_{n,0}$, and the "solutions" given by the algorithm never present a number of undulations larger than n. For every number of cells n, the results are similar to those of Fig. 2 where $n = 16$.

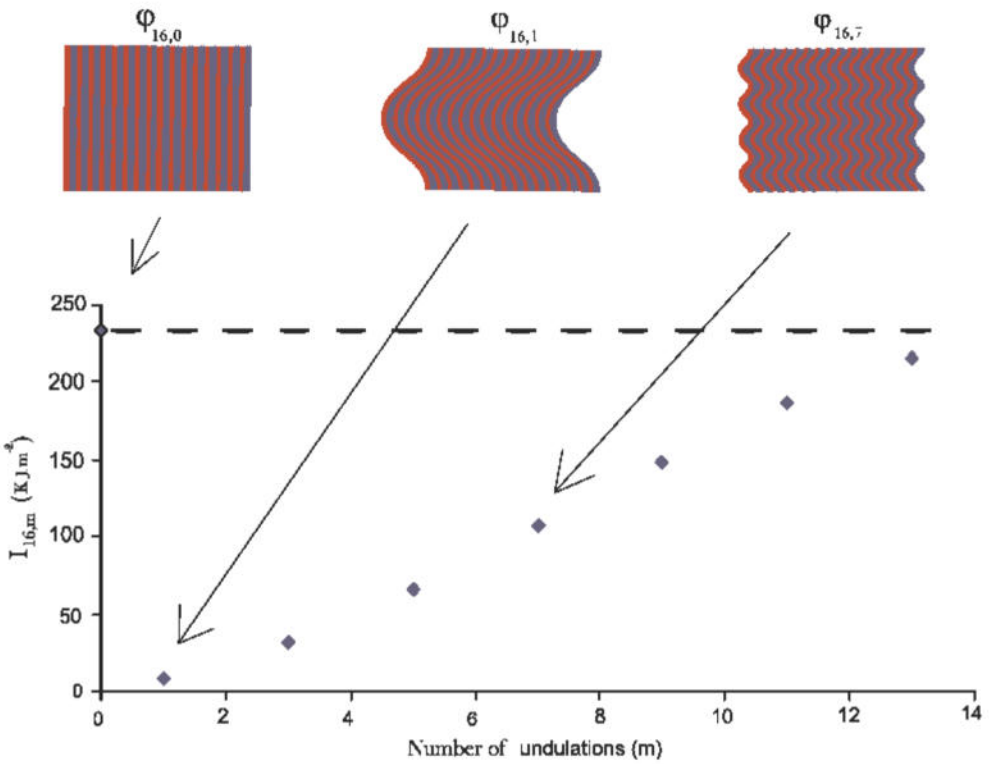

Fig. 2 $\varphi_{16,m}(16Y)$ and $I_{16,m}(F)$ when $d = 0.8$

Table 1 $\overline{I}_n$ for $d = 0.9$

n	1	3	4	5	6	8	12	16	20	32	40
$\overline{I}_n$ $(KJ\,m^{-2})$	57,326	56,804	44,640	32,866	24,576	14,866	6,957	3,985	2,572	1,015	651

Fig. 3 $\overline{I_n}$ for $d = 0.9$

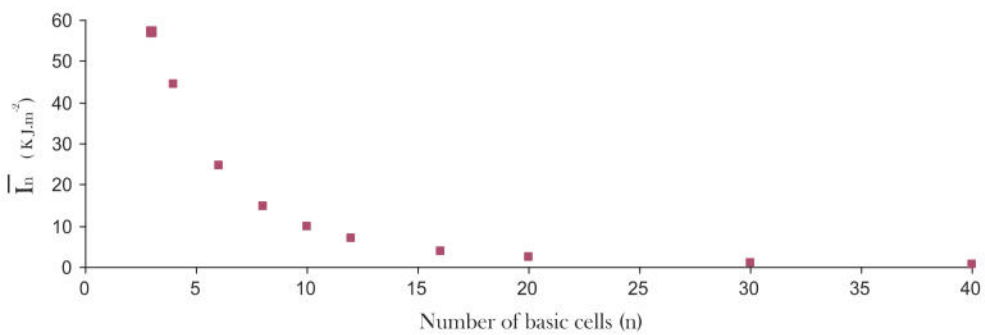

Fig. 4 Two deformed configurations: $\varphi_{10,1}$ (*left*) and $\varphi_{16,1}$ (*right*) for $d = 0.9$

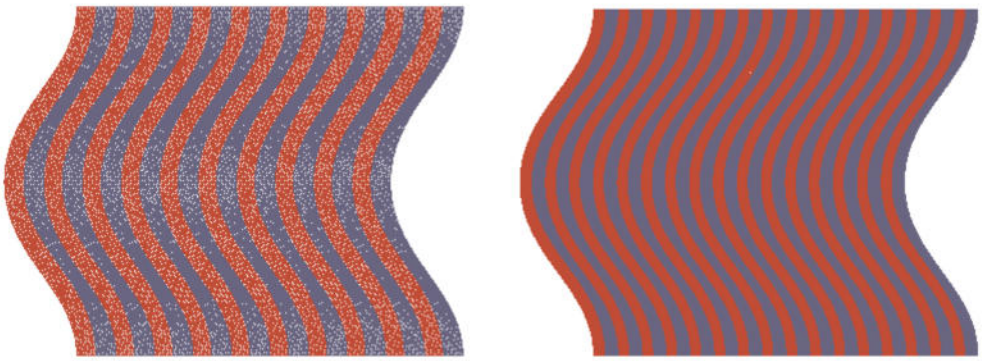

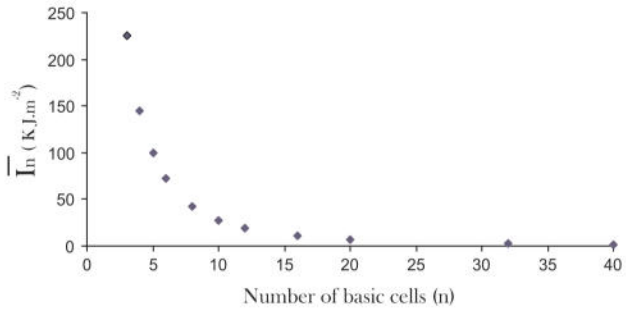

Fig. 5 $\overline{I}_n$ for $d = 0.74$

Table 2 Evolution of $\frac{\overline{I}_1}{\overline{I}_n}$ with d

d	0.9	0.88	0.86	0.84	0.82	0.8	0.78	0.76	74
$\frac{\overline{I}_1}{\overline{I}_n}$	88	105	123	140	157	175	192	209	227

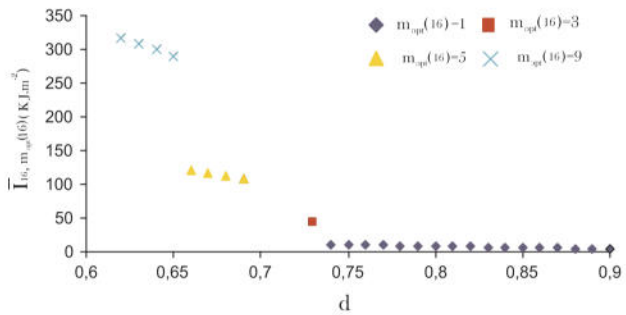

Fig. 6 Evolution of $m_{opt}(16)$ with d

The numerical results reported in Table 1, Figs. 3 and 4 agree with the theoretical results of [11], $\overline{I}_{40}$ is about 90 times lower than $\overline{I}_1$!

In other words, blind use of the "classical" formula (2) would give a homogenized material more than 90 times harder.

In the case of $d = 0.74$, as previously, $\overline{I}_n$ decreases strongly with n (Fig. 5) and using formula (2) would give a homogenized material more than 227 times stronger.

For $d < 0.74$, $m_{\text{opt}}(n)$ decreases with d (Fig. 6).

The algorithm gives deformation fields with several undulations (Figs. 7, 8) and it seems impossible to get "solutions" with few undulations. For instance, with $n = 16$ and $d = 0.7$, the "solution" has at least six undulations. The algorithm stops when the strong layers are close to contact (Figs. 7, 8) and was not possible to consider larger macroscopic deformation gradients.

2.2 Other tests

Next, three types of macroscopic deformation gradients will be considered corresponding first to a normal compression to the layers and next to two shearings:

$$F^1 = \begin{pmatrix} d & 0 \\ 0 & 1 \end{pmatrix},\ F^2 = \begin{pmatrix} 1 & d \\ 0 & 1 \end{pmatrix} \text{ and } F^3 = \begin{pmatrix} 1 & 0 \\ d & 1 \end{pmatrix}.$$

For any values of d, we do not obtain solution with undulations and $\overline{I}_n(F) = \overline{I}_1(F)$, the "solution" $\overline{\varphi}_n$ being built by reproducing $\overline{\varphi}_1$ by periodicity:

2.3 Remarks

In the case of tests like those in Sect. (2.1) and for a fixed value of d, the Newton–Raphson algorithm can provide several solutions with the same level of energy $I_{n,m}$ (Fig. 11).

The shape of the horizontal edges of the deformed unit cell depends on m: flat when m is odd, corrugated when m is even (Figs. 12, 13).

These results stem from the fact that some $\varphi_{n,m}$ can be constructed by elementary transformations of some $\varphi_{n',m'}$ (Figs. 14, 15, 16).

3 Numerical experiments with the Ciarlet–Geymonat density W_{CG}

Now, W_{CG} is the energy density deduced from (6) with $w = w_{CG}$. In the absence of a formula giving the homogenized energy density, tests were carried out directly on a sample of the composite material. So, for a given F, an attempt was made to solve the problem

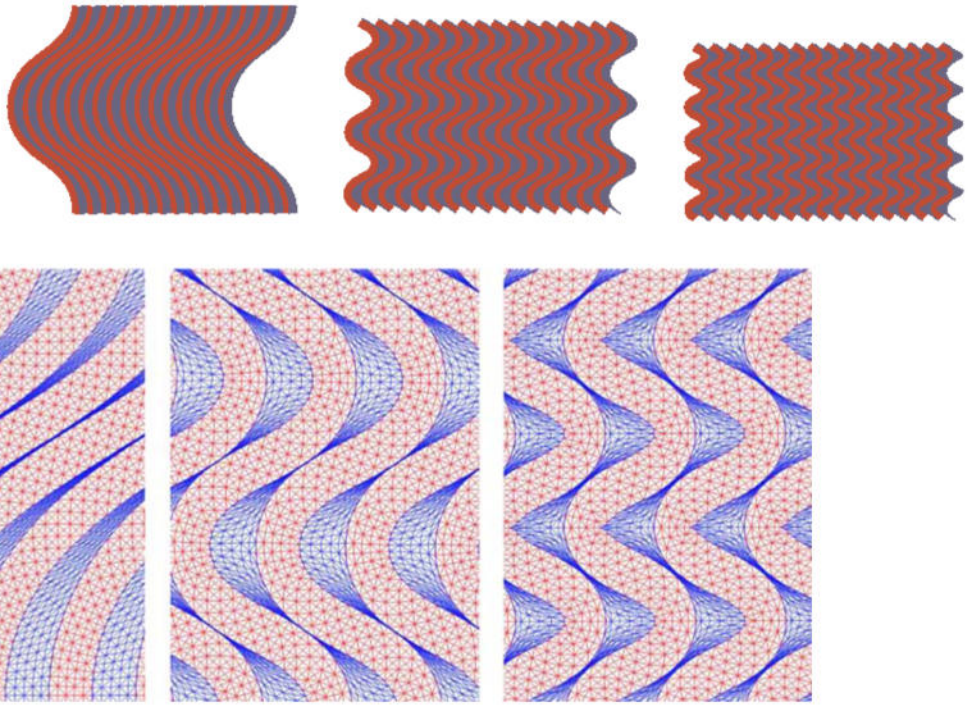

Fig. 7 $\overline{\varphi}_{16}$ when $d = 0.74, 0.7, 0.64$

Fig. 8 Zoom on the "contact zone" between two strong fibers for $\overline{\varphi}_{16}$ when $d = 0.74, 0.7, 0.64$

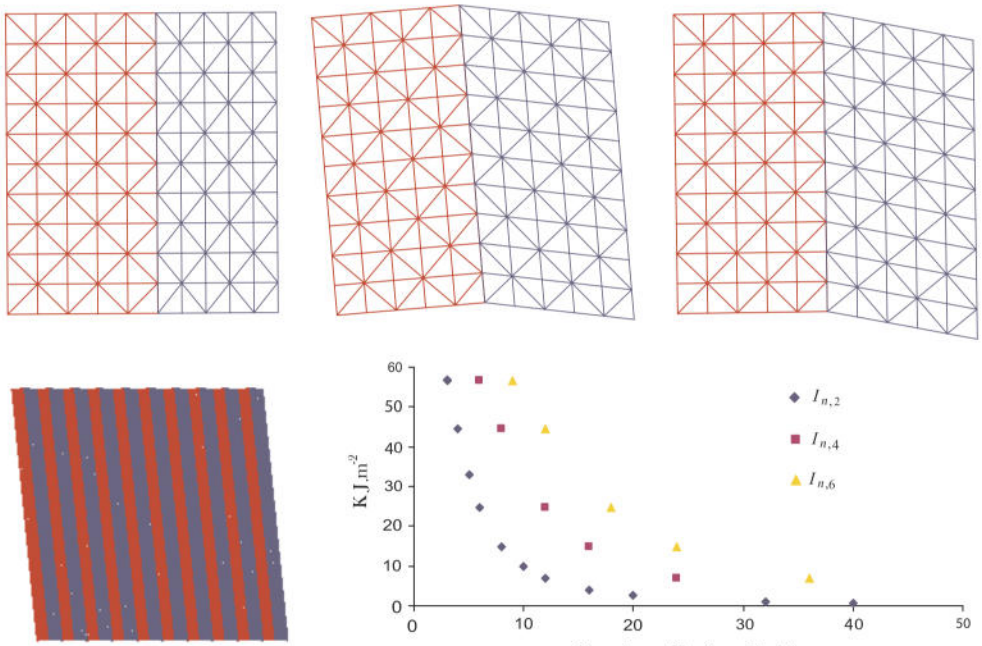

Fig. 9 $\overline{\varphi}_{1,0}$ for F^1 for $d = 0.9$, F^2 and F^3 for $d = -0.1$

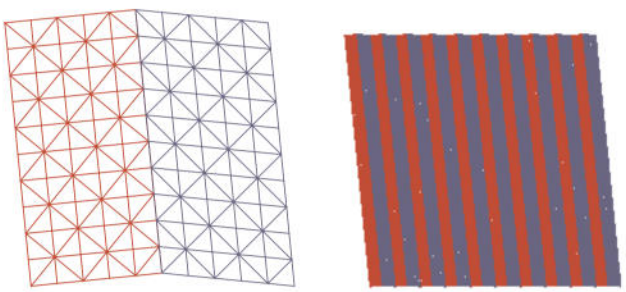

Fig. 10 $\overline{\varphi}_1$ and $\overline{\varphi}_{10}$ for F^2 with $d = -0.1$

Fig. 11 $I_{n,2}$, $I_{n,4}$, $I_{n,6}$ for $d = 0.9$

$$(Q_n) \quad inf \left\{ \frac{1}{|Y|} \int_Y W_{CG}(ny, \nabla\varphi(y))dy, \right.$$
$$\left. \varphi(y) = Fy \quad on \quad \partial Y \right\}$$

numerically, where the function $y \in Y \rightarrow W_{CG}(y, F)$ is extended by Y-periodicity to $\mathbb{R}^2$ and ∂Y denotes the boundary of Y. We expect that when n is very large

$$\overline{W^n} := inf \left\{ \frac{1}{|Y|} \int_Y W_{CG}(ny, \nabla\varphi(y))dy, \right.$$
$$\left. \varphi(y) = Fy \quad on \quad \partial Y \right\}$$

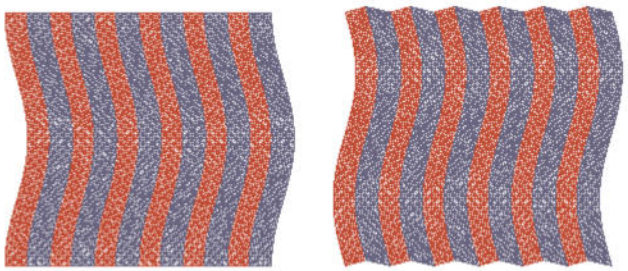

Fig. 12 $\varphi_{6,1}$ and $\varphi_{6,2}$ with $I_{6,1} = I_{6,2}$ for $d = 0.9$

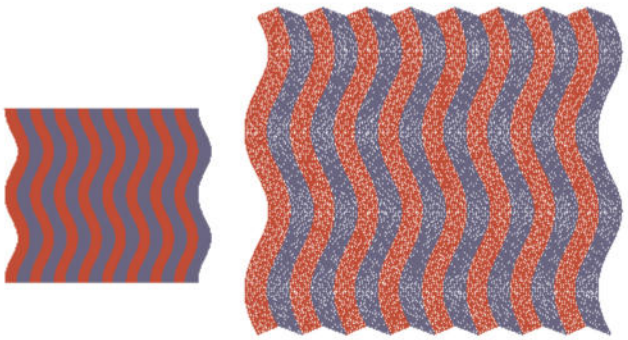

Fig. 13 $\varphi_{8,3}$ and $\varphi_{8,4}$ with $I_{8,3} = I_{8,4}$ for $d = 0.9$

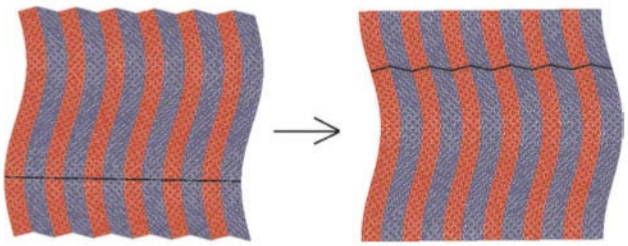

Fig. 14 Construction of $\varphi_{6,1}$ from $\varphi_{6,2}$ for $d = 0.9$

will be a good approximation of the value at F of the homogenized energy density if such a density does exist. Because

$$\overline{W^n}(F) = \quad inf \left\{ \frac{1}{|nY|} \int_{nY} W_{CG}(y, F + \nabla\psi(y))dy, \right.$$
$$\left. \psi(y) = 0 \quad on \quad \partial nY \right\}$$

the numerical problem is similar to that of the previous section. But with this Dirichlet boundary condition on the boundary of nY and for F as in Sect. (2.1), the algorithm is sometimes unable to provide a solution with at least one or more undulations. The use of the Newton–Raphson algorithm with damping [6] allows us to overcome this difficulty for n at least equal to 18. Figure 17 presents the variations with respect to n of the numerical approximation $\overline{J}_n(F)$ of $\overline{W^n}(F)$ and of the optimal number of undulations.

Because $\overline{J}_n$ keeps decreasing for $n = 18$, the following method was used to estimate the value at F of the expected homogenized density. To estimate $\overline{W^{n+1}}(F)$, the field is considered to be $\psi_{\overline{n}}$ which solves the problem (P_n) of Sect. (2.1) (but with Ciarlet–Geymonat energy). Here, $\overline{n}$ is the largest value of n available in the computations with periodicity conditions. Let $\widehat{\psi_n}$ defined on Y by $\widehat{\psi_n}(y) = \frac{1}{\overline{n}}\psi_{\overline{n}}(\overline{n}y)$, it is extended by Y-periodicity to the whole nY set. This extension is modified on the cells adjacent to the boundary ∂nY in order to make it vanish at ∂nY. If $\tilde{\psi}_n$ denotes this modification, then:

$$\tilde{I}_n = \frac{1}{|nY|} \int_{nY} W_{CG}(y, F + \nabla\tilde{\psi}_n)\, dy = \left(\frac{n}{n+1}\right)^2 \overline{I}_{\overline{n}} + l_n$$

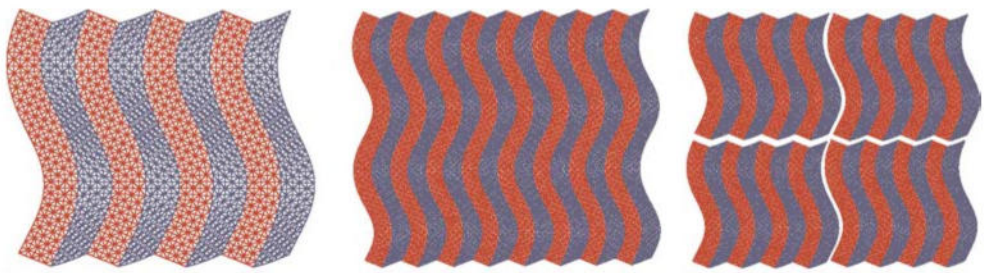

Fig. 15 $\varphi_{8,4}$ can be constructed with the replication of $\varphi_{4,2}$

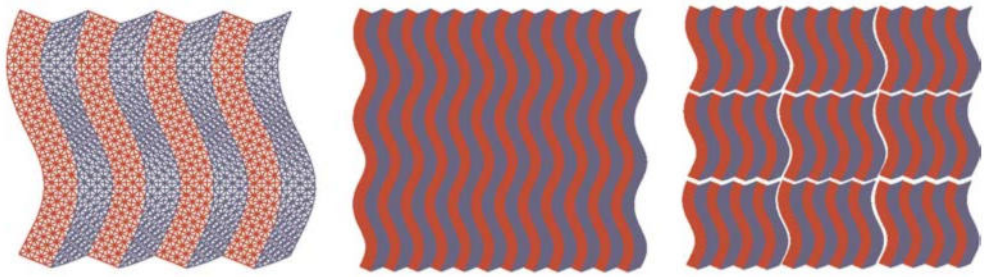

Fig. 16 $\varphi_{12,6}$ can be constructed with the replication of $\varphi_{4,2}$

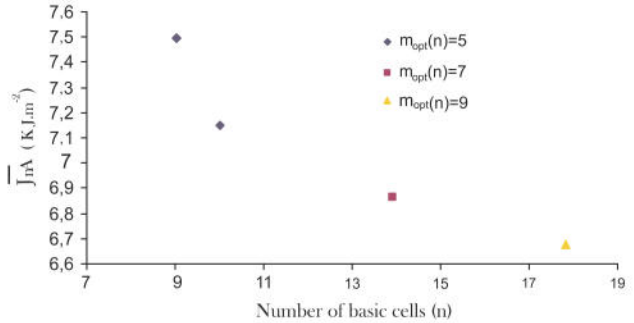

Fig. 17 Evolution of $\overline{J}_n$ with n for $d = 0.9$

where l_n is of the order of $\frac{1}{n}$. Because, clearly, $\overline{W^n}(F) \leq \tilde{I}_n(F)$, we deduce that $\overline{I}_{\overline{n}}$ is an upper bound of the value at F of the expected homogenized density. A formula like (4) will probably give an upper bound of the homogenized energy density if it does exist...

Anyway, here again, the approximation by only considering periodic fields in cell Y produces a far stronger material, here more than 90 times greater for $d = 0.9$ and 250 times for $d = 0.74$!

Remark For smaller values of d, it is necessary to consider a greater number of basic cell to get a very small value of $\overline{I}_n$. For purely numerical problems this phenomenon could not be emphasized.

Remark For a fixed value of d, the numerical solutions obtained with m undulations and $\overline{n}$ basic cells practically have two hard layers in contact. The solution towards which Newton–Raphson converges has a greater number of undulations. This remark is valid only in the case of Dirichlet boundary conditions.

4 Conclusion

The numerical simulations of large deformations of heterogeneous hyperelastic media presented in this paper highlight the considerable difference between the expressions (2) and (4) for possible macroscopic stored energy densities. The formula (2) substantially overestimates the stiffness, while a large number of multiples of the basic cell are required to get an estimation of the homogeneous density through the formula (4). This discrepancy can be explained in our example of composite by micro-scale bucklings which are characteristically difficult to trap numerically. For instance, in the case of Ciarlet–Geymonat density which needs to consider Dirichlet boundary conditions, the Newton–Raphson algorithm had to be improved. Therefore much remains to be done from the algorithm point of view. Moreover, it is interesting to consider other heterogeneous media, where significant micro-scale deformations may occur: for instance the honeycomb

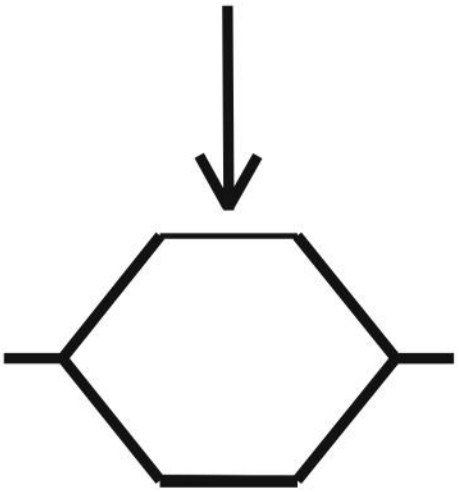

Fig. 18 The unit cell and loading

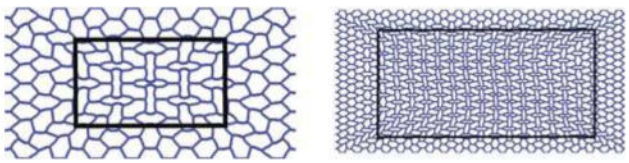

Fig. 19 **a** $n = 20$ and $d = 0.8$, **b** $n = 20$ and $d = 0.8$

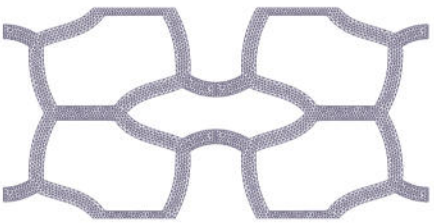

Fig. 20 Periodic "solution" for $n = 2$ and $d = 0.8$

cellular media is a suitable model for wood material. The numerical experiments will be done with energy density W_{CG} and a macroscopic deformation gradient corresponding to a so-called radial compression (Fig. 18).

As explained in Sect. (3), tests were carried out directly on a cellular media subjected to Dirichlet boundary conditions. The "solution" obtained for $n = 8$ and $n = 20$ and for $d = 0.8$ is given in Fig. 19. Note that when n increases, the solution is close to the periodic one in the centre of the specimen. Thus, it can be postulated that the homogenized energy density is given by considering two unit cells and periodic boundary conditions (Fig. 20). An interesting extension of this study will be to consider the self-contact of the cell walls [1,12].

References

1. Barboteu M, Alart P, Pagano S (2002) Modélisation de problèmes non linéaires de grande taille : grandes déformations et autocontact dans un milieu cellulaire. Revue Européenne des Eléments 2-3-4:447–461
2. Bensoussan A, Lions J, Papanicolaou G (1978) Asymptotic analysis for periodic structures. North-Holland, Amsterdam
3. Braides A (1985) Homogenization of some almost periodic coercive functionals. Rend Accad Naz XL 9:313–322
4. Ciarlet P (1988) Three-dimensional elasticity. North-Holland, Amsterdam
5. Ciarlet P, Geymonat G (1982) Sur les lois de comportement en élasticité non linéaire compressible. CR Acad Sci Paris Série II 295:423–426
6. Curnier A (1993) Méthodes numériques en mécanique des solides, 1st edn. Presses polytechniques et universitaires romandes, Suisse
7. Debordes O (2001) Cours sur l'homogénéisation périodique. Tech. rep., EGIM, Marseille
8. Dhatt G, Touzot G (1984) Une présentation de la méthode des éléments finis, 2nd edn. Maloine S.A., Paris
9. Duvaut G (1978) Analyse fonctionnelle et mécanique des milieux continus, applications à l'étude des matériaux composites élastiques à structure périodique, homogénéisation. In: Koiter W (ed) Theoretical and applied mechanics. North-Holland, Amsterdam pp 119–131
10. Marcellini P (1978) Periodic solution and homogenization of non linear variationnal problems. Math Mod Num Anal 28:139–152
11. Müller S (1987) Homogeneization of non convex integral functionals and cellular elastic materials. Arch Rational Mech Anal 99:198–212
12. Pagano S, Alart P (2007) Self-contact and fictitious domain by a difference convex approach. Int J Numer Methods Eng (in press)
13. Sanchez-Palencia E (1980) Non-homogeneous media and vibration theory. No. 127 in Lect. Notes in Physics, Heidelberg
14. Suquet P (1982) Plasticité et homogénéisation. Thèse de doctorat d'état, Université Pierre et Marie Curie
15. Tartar L (1977) Problèmes d'homogénéisation dans les équations aux dérivées partielles. Tech Rep, Cours Peccot, Collège de France, Paris